

## Original article

## 3D-QSAR, Synthesis, and antimicrobial activity of 1-Alkylpyridinium Compounds as Potential Agents to Improve Food Safety

Sergio Rodríguez-Morales <sup>a,\*</sup>, R. Lilia Compadre <sup>b</sup>, Rafael Castillo <sup>a</sup>,  
Philip J. Breen <sup>b</sup>, Cesar M. Compadre <sup>b</sup><sup>a</sup> Departamento de Farmacia, Facultad de Química UNAM, CU Mexico, DF 04510, Mexico<sup>b</sup> Department of Pharmaceutical Sciences, University of Arkansas for Medical Sciences, Little Rock, Arkansas 72205, USA

Received 26 March 2004; received in revised form 1 February 2005; accepted 3 February 2005

Available online 28 April 2005

## Abstract

Cetylpyridinium chloride (CPC), an alkylpyridinium compound has been recently approved by the US Food and Drug Administration to reduce bacterial contamination in poultry. Although CPC is very effective and has a very good safety record, its relatively high lipophilicity may limit its use in high fat containing foods such as beef. In this study we present the CoMFA analysis (3D-QSAR) of the antimicrobial activity of 60 *N*-alkylpyridinium compounds against different bacteria. CoMFA contours showed that the activity is highly influenced by the steric factor. Based in these contours we designed new candidates, which were synthesized and characterized by spectroscopic data. MIC activity over Gram positive and Gram negative microorganisms validated the 3D-QSAR study.

© 2005 Elsevier SAS. All rights reserved.

**Keywords:** Cetylpyridinium chloride; Alkylpyridinium analogues; 3D-QSAR; CoMFA analysis; MIC activity

## 1. Introduction

Foodborne diseases are one of the mayor concerns around the world. While the American food supply is considered among the safest in the world, recent estimates suggest that as many as 9,000 deaths and 6.5 to 33 million illnesses in the United States each year are food-related. Medical costs and productivity losses range between \$1.8 billion and \$4.8 billion annually [1]. The need to develop strategies to eliminate and prevent microbial contamination of food products is made more urgent by the appearance of new strains and types of food pathogens, new and more frequent outbreaks of foodborne disease, and the increased susceptibility to foodborne infections in population groups with lowered immunity [2].

In this context we have demonstrated that cetylpyridinium chloride (CPC), a chemical safely used for more than 50 years in oral hygiene products, can reduce *Salmonella* and other bacterial contamination in poultry, meat, fish, fresh fruits, and vegetables [3]. CPC is also effective in preventing bacterial

attachment and thus, has potential to reduce the risk of cross-contamination [3,4]. Furthermore, CPC has been recently approved by the US Food and Drug Administration to reduce bacterial contamination in poultry. Although CPC is very effective and has been safely used in the pharmaceutical field as a mouthwash, its relatively high chemical residue in some foods products, such as beef, may limit its acceptance by the consumer [5]. Recently, polymeric quaternary ammonium derivatives have been used as bacteria killing surfaces [6–8].

In an effort to develop CPC analogues that could be easily removed from food products after treatment, we have developed a systematic study of quantitative structure activity relationships (QSAR) of CPC and its analogues using 2D-QSAR and 3D-QSAR techniques. Previous SAR studies for these compounds have shown that the antimicrobial activity is significantly affected by the substituents on the pyridine moiety, the length of the alkyl chain, the hydrophobicity of the compound, their absorbability on the cell, and the pK<sub>a</sub> of the parent pyridine [9–13]. However, these studies were performed in individual subsets of pyridinium compounds, and no effort has been made to generate an overall picture of the SAR or quantitative SAR (QSAR) for these compounds.

\* Corresponding author: Lab 122, Departamento de Farmacia, Facultad de Química UNAM, CU, DF 04510, Mexico. Fax: (525) 56225329.

E-mail address: [rafaelc@servidor.unam.mx](mailto:rafaelc@servidor.unam.mx) (R. Castillo).

Among 3D-QSAR methods [14], Comparative Molecular Field Analysis (CoMFA) is widely applied on the medicinal chemistry field. Comprehensive reviews [14,15], criteria for derivation of the models [16], guidelines for publishing [17], and scope and limitations [18] of the method have been published.

In this paper we report the QSAR analysis (2D and 3D-QSAR) of the antimicrobial activity of 60 *N*-alkylpyridinium compounds against *Escherichia coli*, *Staphylococcus aureus*, *Pseudomonas aeruginosa*, *Klebsiella pneumoniae*, *Bacillus subtilis*, and *Bacillus megaterium*. Also, we present the synthesis of the analogues that were selected, and the antimicrobial activity, which validated the CoMFA models generated.

## 2. Chemistry

### 2.1. Molecular modeling studies

#### 2.1.1. Biological Data

A data set of 60 antimicrobial activities (Minimum Inhibitory Concentration (MIC)) and the logarithm of the octanol water partition coefficients (log *P*) were retrieved from the literature [5,9,10,19–21]. For the analysis, the antimicrobial activities are expressed as the LOGMIC (LOGMIC = log 1/MIC).

#### 2.1.2. Molecule 3D-Building

The structures of the compounds were obtained from the Cambridge Crystallographic Database as implemented in Unity 4.1 or by small modifications of structures available in the database using Sybyl 6.8. All the analogues were minimized by the PM3 semiempirical Hamiltonian in MOPAC 6.0 package in Sybyl (keywords used: Precise, Full, Mullik and in some cases MMOK). After minimization, the following descriptors were retrieved from the output file: Dipolar Moment (DM), Highest Occupied Molecular Orbital (HOMO), Lowest Unoccupied Molecular Orbital (LUMO), Ionization Potential (IP), and Heat of formation (DHF). These data are shown in Table 2.

#### 2.1.3. QSAR Analysis

Classical QSAR (2D-QSAR) studies were performed using the CoMFA module in Sybyl 6.8. The compounds included in this study, the antimicrobial activity, as well as the descriptors obtained after minimization, are listed in Tables 1 and 2.

#### 2.1.4. Comparative Molecular Field Analysis (CoMFA)

3D-QSAR studies were performed using the program CoMFA analysis as implemented in SYBYL 6.8 molecular

modeling software from Tripos Inc., St. Louis, MO (Tripos, 2002). See experimental protocols for full details.

### 2.2. Synthesis of the analogues selected

Target alkylpyridinium compounds were synthesized according to reaction shown in Scheme 1. The proper substituted pyridine was reacted with the corresponding alkyl bromide (for derivatives with a 12-C chain) or alkyl tosylate (for derivatives with a 16-C chain) in equimolar quantities in a suitable solvent, under 200 PSI of nitrogen in a 300 ml Parr reactor (Parr instruments, Ill. USA). After the time of reaction, the solvent was evaporated under vacuum, and 100 ml of ether were added. The reaction mixture was chilled at 0 °C for 10–12 h, and the solid obtained was filtered and dried. Isolation of the compounds was performed by a flash chromatography column technique [22], using chloroform:methanol in a gradient of 0 to 10% (increments of 1% every 300 ml of mobile phase) and silica gel deactivated with 12% NaBr, as mobile and stationary phase respectively. After separation, the counter ion was exchanged for a bromide ion; so, most of the final compounds are alkylpyridinium bromides. All the synthesized compounds are very hygroscopic and newly described, except for compound 12 [5]. Reaction conditions and physicochemical data of these compounds are shown in Table 3. Elemental analysis, for C, H, N, were within the range  $\pm 0.4\%$  of theoretical values. Structural IR,  $^1\text{H}$  NMR and  $^{13}\text{C}$  NMR data for compounds 3 are given in full detail in the experimental protocol. Complete data for the other compounds can be obtained from the authors on request.

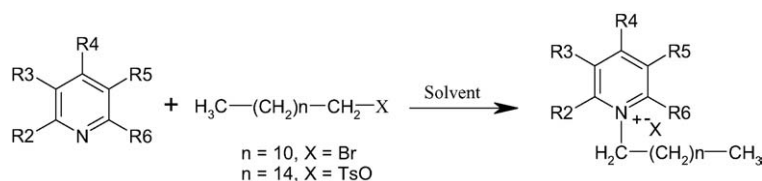
## 3. Biology

### 3.1. Partition coefficient (log *P*) determination

Log *P* octanol/water was measured using the guidelines of Hansch and Leo [23].

### 3.2. Antimicrobiological activity

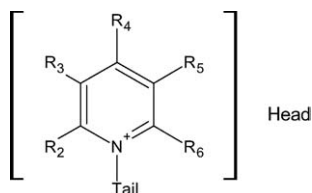
Minimum Inhibitory Concentration (MIC) against *Salmonella typhimurium* ATCC 14028, *E. coli* ATCC25922, *S. aureus* ATCC29123 was determined as antimicrobial activity using the macrodilution method, as reported in the literature [24]; CPC and ampicillin were used as controls.



Scheme 1.

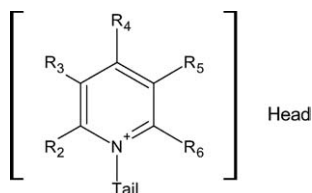
Table 1

Log P and antimicrobial activity of N-Alkylpyridinium compounds reported in the literature



Compound		MIC (log 1/IC50)						
Tail Nr C	Head substituent	<i>B. subtilis</i>	<i>B. megaterium</i>	<i>S. aureus</i>	<i>E. coli</i>	<i>P. aeruginosa</i>	<i>K. pneumoniae</i>	LOGP
16	2-methyl	6.17	5.57	6.66	4.75	4.01	5.57	1.95
16	2,4-dimethyl	6.19	6.00	6.70	5.19	3.82	5.28	3.90
16	3-carbamoyl	5.68	4.92	5.77	4.68	3.89	4.82	1.44
16	3,4-dimethyl	6.19	5.89	6.59	5.19	3.89	6.06	3.16
16	3,5-methyl	5.19	5.96	6.89	5.19	3.96	6.00	3.35
16	3-niketamide			2.22	2.48			
16	4-butenyl	6.13		5.52	5.23		5.82	
16	Unsubstituted	6.04	5.75	6.64	5.04	4.06	5.75	2.81
10	2-methyl	4.26	4.09	4.85	3.68	3.26	4.39	0.19
10	2,4-dimethyl	4.57	4.57	5.00	3.70	3.10	4.80	0.54
10	3-carbamoyl	3.72	4.05	4.50	3.29	3.29	4.19	-0.29
10	3,4-dimethyl	4.57	4.57	5.10	3.80	3.10	4.68	0.66
10	3,5-dimethyl	4.28	4.40	4.96	3.62	3.17	4.57	0.76
10	3-DEAC <sup>a</sup>			2.48	2.56			
10	4-butenyl	4.13		4.13	4.13		3.83	
10	Unsubstituted	3.96	4.07	5.07	3.70	3.15	4.24	0.11
12	2,4,6-trimethyl	6.41			5.59			1.41
12	2,4-dimethyl	5.52	5.52	5.92	4.40	3.52	5.66	1.44
12	2,6-dimethyl	5.30			4.70			2.05
12	2-amino	5.00			4.36			0.95
12	2-carboxyl	3.42			2.96			0.64
12	2-cyano	5.55			4.56			0.00
12	2-ethyl	4.92			4.35			1.34
12	2-methyl	5.29	5.00	6.11	4.39	3.82	5.00	1.32
12	2-propyl	5.20			4.62			1.75
12	3,4-dimethyl	5.40	5.52	5.92	4.30	3.52	5.43	1.91
12	3,5-dimethyl	5.30	5.40	5.92	4.30	3.60	5.28	1.92
12	3-amino	5.74			4.54			0.60
12	3-carbamoyl	4.62	4.72	5.32	4.07	3.77	4.62	0.60
12	3-carboxyl	3.55			3.11			-0.17
12	3-cyano				3.87			0.00
12	3-methyl	5.31			4.29			1.21
12	4-amino	5.80			5.00			
12	4-butenyl	5.60		5.29	4.69		5.28	0.05
12	4-carbamoyl	4.62			4.08			0.63
12	4-carboxyl	3.46			3.00			0.09
12	4-cyano				3.76			0.00
12	4-methyl	5.34			4.51			
12	Unsubstituted	4.96	3.96	5.80	4.60	3.62	4.96	2.15
14	2-methyl	6.15	5.62	6.44	4.92	4.26	5.44	2.27
14	2,4-dimethyl	6.03	6.03	6.60	4.85	4.16	6.13	2.47
14	3-carbamoyl	5.35	5.35	6.05	4.75	4.31	5.35	1.14
14	3,4-dimethyl	6.03	5.92	6.38	4.92	4.03	6.03	2.93
14	3,5-dimethyl	6.03	5.92	6.64	4.92	4.03	6.08	2.90
14	3-DEAC <sup>a</sup>			2.25	2.42			
14	4-butenyl	5.62		5.32	5.02		5.33	
14	Unsubstituted	5.82	5.70	6.52	4.82	4.05	5.70	3.56
8	2-methyl	3.35	3.05	3.92	3.13	2.75	3.35	-0.77
8	2,4-dimethyl	4.46	3.46	4.13	3.22	2.85	3.54	-0.57

(continued on next page)

Table 1  
(continued)

Compound		MIC (log 1/IC50)						
8	3-carbamoyl	2.85	2.96	3.39	2.85	2.89	2.95	-0.70
8	3,4-dimethyl	3.64	4.77	4.24	3.46	2.70	3.64	-0.41
8	3,5-dimethyl	3.16	3.46	3.92	3.16	2.70	3.54	-0.17
8	3-DEAC <sup>a</sup>			2.57	2.59			
8	4-butenyl	3.25	2.95	3.85	3.25		3.25	
8	Unsubstituted	3.04	3.07	3.96	3.08	2.60	3.21	-0.08
18	2-methyl	6.08	5.52	6.38	4.77	4.89	5.50	2.48
18	2,4-dimethyl	6.09	5.60	6.60	4.80	3.85	5.75	3.73
18	3-carbamoyl	5.62	4.80	5.80	4.40	3.80	4.80	1.93
18	3,4-dimethyl	5.92	5.60	6.39	4.92	3.54	5.68	3.17
18	3,5-dimethyl	5.92	5.60	6.68	5.09	3.68	5.54	3.16
18	3-DEAC <sup>a</sup>			2.29	2.57			
18	4-butenyl	5.36		4.75	4.45		4.75	
18	Unsubstituted	5.66	4.82	6.52	4.59	4.00	5.37	3.68

<sup>a</sup> (Diethylamino)carbonyl.

## 4. Results and discussion

### 4.1. 2D-QSAR studies

For the molecular modeling study, an extensive search of the literature was performed. Nearly 60 molecules were found with different substitution patterns in the pyridine head and / or the linear carbon chain. All the molecules for the training set are presented in Table 1. There are more molecules reported in the literature; but their activity was determined using the disc method, which precluded their use in this study. Most of the molecules in Table 1 were found in the crystallographic database Unity 4.1. The crystal structure was minimized directly with the semiempirical PM3 algorithm. Only dimethyl, trimethyl, and amido derivatives were modeled by small modifications of the corresponding analogue and then minimized by PM3 methodology. After the minimization process, some descriptors were retrieved from calculations (dipolar moment, heat of formation, the Lowest Unoccupied Molecular Orbital, and the Highest Occupied Molecular Orbital) and others were taken from the literature (LogP). Table 2 summarizes the descriptors retrieved from calculations. Using these data, a correlation matrix was calculated to find the correlation, as well as the colinearity, between descriptors (Table 4). Results indicate that only the LogP describes the antimicrobial activity, as is seen in equation 1 for *E. coli*, and in equation 2 for *S. aureus*:

$$\text{LogMIC}_{B.\text{subtilis}} = 0.634 (0.125) \log P + 4.115 (0.245) \quad (1)$$

(n = 49, r = 0.846, s = 0.533)

$$\text{LogMIC}_{E.\text{coli}} = 0.468 (0.087) \log P + 3.592 (0.171) \quad (2)$$

(n = 49, r = 0.874, s = 0.347)

In these equations, n is the number of data points used in the regression analysis, r is the correlation coefficient and s is the standard deviation. On the other hand, Mopac descriptors are poorly correlated and did not increment the statistical significance when added to the equation.

In search for a better model, a bilinear and parabolic model was computed in the same dataset. Equations 3 and 4 show the results for a good correlation between the LogP and MIC with the bilinear model.

$$\text{LogMIC}_{B.\text{subtilis}} = 1.131 (0.239) \log P - 1.150 (0.498) \text{BILIN} (\log P) + 3.934 (0.220) \quad (3)$$

$$\text{LogP optimum} = 3.548, \log (\beta) = -1.788 \quad n = 49, r = 0.904, s = 0.443$$

$$\text{LogMIC}_{E.\text{coli}} = 0.825 (0.180) \log P - 0.759 (0.349) \text{BILIN} (\log P) + 3.475 (0.156) \quad (4)$$

$\log (\beta) = -1.651$

The slopes and intercepts in the equations show the fact that Gram positive bacteria are generally more sensitive to the alkylpyridinium compounds than the Gram negative bacteria, as Lien and coworkers has demonstrated [25].

In general, the models are significant, with an r = 0.85 for the lowest correlation model. Although these equations could be used in predicting the antimicrobial activity of new compounds, computational calculation of the LogP for the alky-

Table 2  
Descriptors calculated for the alkylpyridinium compounds in Mopac

Compound		Descriptors				
Tail Nr	Head	MD <sup>a</sup>	DH <sup>a</sup>	HOMO <sup>a</sup>	LUMO <sup>a</sup>	PI
C	Substituent.					
16	2-methyl	1.89	-51.62	-9.71	-3.31	6.66
16	2,4-dimethyl	1.75	-61.06	-9.61	-3.29	6.58
16	3-carbamoyl	3.92	-48.85	-9.57	-3.51	6.92
16	3,4-dimethyl	1.62	-61.19	-9.49	-3.26	6.60
16	3,5-methyl	1.62	-28.95	-9.55	-3.24	6.64
16	3-DEAC <sup>b</sup>	1.75	-36.94	-9.69	-3.33	6.67
16	4-butenyl	1.91	-43.17	-9.98	-3.32	6.73
16	Unsubstituted	1.91	-19.05	-9.72	-3.29	6.65
10	2-methyl	1.77	-28.49	-9.61	-3.27	6.58
10	2,4-dimethyl	3.92	-48.85	-9.57	-3.51	6.92
10	3-carbamoyl	1.64	-27.94	-9.48	-3.26	6.60
10	3,4-dimethyl	1.62	-28.95	-9.55	-3.24	6.64
10	3,5-dimethyl	1.92	-9.36	-9.68	-3.06	6.47
10	3-niketamide	1.91	-10.64	-9.97	-3.32	6.72
10	4-butenyl	1.92	-47.7	-9.53	-3.17	6.45
10	Unsubstituted	1.73	-39.31	-9.6	-3.29	6.59
12	2,4,6-trimethyl	1.99	-38.4	-9.53	-3.20	6.54
12	2,4-dimethyl	1.52	-28.82	-8.63	-3.04	6.52
12	2,6-dimethyl	5.32	-114.71	-10.37	-3.98	7.21
12	2-amino	4.04	13.41	-10.24	-4.01	7.27
12	2-carboxyl	1.88	-35.64	-9.76	-3.32	6.67
12	2-cyano	1.89	-29.93	-9.71	-3.31	6.66
12	2-ethyl	1.89	-39.95	-9.72	-3.28	6.64
12	2-methyl	1.64	-38.78	-9.48	-3.26	6.60
12	2-propyl	1.64	-39.75	-9.56	-3.23	6.63
12	3,4-dimethyl	1.52	-28.82	-8.63	-3.04	6.52
12	3,5-dimethyl	1.52	-28.82	-8.63	-3.04	6.52
12	3-amino	3.01	-111.09	-10.32	-3.65	7.04
12	3-carbamoyl	5.08	26.17	-10.22	-3.74	7.14
12	3-carboxyl	1.79	-30.3	-9.64	-3.25	6.66
12	3-cyano	2.21	-22.97	-8.79	-3.22	7.04
12	3-methyl	1.75	-15.29	-9.69	-3.32	6.66
12	4-amino	5.47	-61.14	-9.31	-3.76	7.04
12	4-butenyl	5.29	-114.71	-10.37	-3.99	7.22
12	4-carbamoyl	6.63	10.85	-10.22	-4.02	7.23
12	4-carboxyl	1.76	-30.98	-9.68	-3.31	6.65
12	4-cyano	1.91	-21.49	-9.98	-3.32	6.72
12	4-methyl	1.88	-40.77	-9.71	-3.31	6.66
12	Unsubstituted	1.73	-50.21	-9.61	-3.29	6.59
14	2-methyl	2.97	-70.5	-9.57	-3.54	6.95
14	2,4-dimethyl	1.86	-56.33	-9.43	-3.01	6.42
14	3-carbamoyl	1.66	-50.55	-9.56	-3.21	6.62
14	3,4-dimethyl	1.76	-26.12	-9.69	-3.32	6.66
14	3,5-dimethyl	1.93	-32.32	-9.97	-3.31	6.72
14	3-DEAC <sup>b</sup>	1.91	-8.21	-9.72	-3.29	6.65
14	4-butenyl	1.76	-17.65	-9.61	-3.28	6.58
14	Unsubstituted	3.89	-37.95	-9.57	-3.51	6.92
8	2-methyl	1.65	-17.09	-9.47	-3.25	6.59
8	2,4-dimethyl	1.61	-18.11	-9.55	-3.24	6.64
8	3-carbamoyl	1.75	6.44	-9.68	-3.32	6.66
8	3,4-dimethyl	1.91	0.19	-9.97	-3.32	6.72
8	3,5-dimethyl	1.92	-62.41	-9.72	-3.29	6.65
8	3-DEAC <sup>b</sup>	1.78	-71.86	-9.61	-3.27	6.58
8	4-butenyl	3.93	-92.17	-9.57	-3.52	6.92
8	Unsubstituted	1.62	-72.03	-9.48	-3.26	6.59
18	2-methyl	1.62	-72.3	-9.55	-3.24	6.63
18	2,4-dimethyl	1.76	-47.79	-9.69	-3.32	6.66

Compound		Descriptors				
18	3-carbamoyl	1.91	-54.01	-9.98	-3.32	6.73
18	3,4-dimethyl	6.63	10.85	-10.22	-4.02	7.23
18	3,5-dimethyl	1.76	-30.98	-9.68	-3.31	6.65
18	3-DEAC <sup>b</sup>	1.91	-21.49	-9.98	-3.32	6.72
18	4-butenyl	1.88	-40.77	-9.71	-3.31	6.66
18	Unsubstituted	1.73	-50.21	-9.61	-3.29	6.59

<sup>a</sup> Mopac en Sybyl6.8.

<sup>b</sup> (Diethylaminocarbonyl).

lpyridinium is not possible, because the positive charge in the pyridine group introduces a variation which is difficult to predict. Since a systematic study was implied in the beginning of this study, a migration to the 3D-QSAR was pursued [16] since the descriptors are generated in the 3D structure of each ligand.

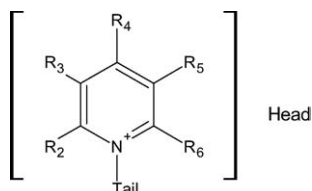
#### 4.2. 3D-QSAR studies

In this part of the study, all the molecules selected from the literature were aligned using CPC as template. After alignment, CoMFA routine was performed over the 60 molecules of the dataset. Then, predictability was measured by the cross validated (Leave-one-out) PLS methodology, and the linearity by the PLS non validated. The results are presented in Table 5. The CoMFA analyses reported in Table 5 are statistically significant, the validated correlation is high ( $q > 0.6$ ) and the linearity is good in all of the models, except for those of *E. coli* and *B. subtilis*, which have the lowest linearity and predictability possible due to the larger number of compounds used in the derivation (60 and 55, respectively). However, these results are more relevant since they include variation in both the pyridine substituents and in the alkyl chain. Figs. 1,2 show the steric and the electronic CoMFA contours for Gram negative (*E. coli*) and Gram positive (*S. aureus*) bacteria, respectively. The steric dependency of the antimicrobial activity is notable in these figures. For the alkyl chain, the activity is increased when the length of the chain is 14–16 carbons (green contours) and the activity is decreased when the length is more than 18 carbons (yellow contours), as reported [9–11,13]. Unexpectedly, the steric effect of substituents on the pyridine head also has a large influence on activity. According to the CoMFA analysis, bulky groups are allowed at position 2 of the pyridine moiety (green contour), but they should be avoided on the other positions (yellow contours) for the activity to be increased. In this models electrostatic effects were not evident, with the exception of small contribution on the *S. aureus* (5%).

CoMFA analysis could be used to predict the activity of new candidate compounds prior to their synthesis, and this new information is used to validate the model. Table 6 summarizes the results for all of the candidates. The synthetic strategy was based on the models for Gram negative bacteria, because of their relevance in food safety, for example *E. coli* and *Salmonella typhimurium* that are major concerns. Based on the CoMFA contours in the first part of the study hydroxymethyl, methoxy, acetyl and methyl groups were con-



Table 3  
Reaction conditions for the synthesis of the analogues selected



	Tail Nr C	Head Pyridine Subst.	Analysis (C, H, N)	m.p. °C	Yield %	Press (PSI)	Temp °C	Time (h)
	16C	4-acetyl	C <sub>23</sub> H <sub>40</sub> BrNO	88–89	37	150	130 <sup>a</sup>	26
<b>10</b>	16C	2,4,6-trimethyl	C <sub>24</sub> H <sub>44</sub> BrN	106–107	35	150	132 <sup>a</sup>	192
<b>11</b>	12C	4-acetyl	C <sub>19</sub> H <sub>32</sub> BrNO	82–83	56	50	100 <sup>b</sup>	27
<b>12</b>	12C	2,4,6-trimethyl	C <sub>20</sub> H <sub>36</sub> BrN	92–94	20	NP	83 <sup>a</sup>	336
<b>14</b>	16C	4-(methyloxy)methyl	C <sub>23</sub> H <sub>42</sub> BrNO	72–76	32	150	130 <sup>a</sup>	26
<b>18</b>	12C	4-(methyloxy)methyl	C <sub>19</sub> H <sub>34</sub> BrNO	69–70	35	150	130 <sup>a</sup>	192
<b>19</b>	16C	3,4-dimethylhydroxy-5-hydroxy-2-methyl	C <sub>31</sub> H <sub>51</sub> NO <sub>6</sub> <sup>c</sup>	118–120	37	200	100 <sup>b</sup>	27

<sup>a</sup> Acetonitrile.

<sup>b</sup> Ethanol.

<sup>c</sup> crystallizes as tosylate.

Table 4  
Correlation matrix between the MIC over different bacteria and molecular descriptor for the alkylpyridinium compounds

	E.coli	B. subtilis	B. megaterium	S. aureus	Ps. aeruginosa	K. pneumoniae	LogP	M.D	DH <sub>f</sub>	HOMO	Pot. Ion	LUMO
<i>E. coli</i>	1.0000											
<i>B. subtilis</i>	0.9428	1.0000										
<i>B. megaterium</i>	0.9114	0.9015	1.0000									
<i>S. aureus</i>	0.9068	0.9082	0.9224	1.0000								
<i>Ps. aeruginosa</i>	0.8545	0.8377	0.7898	0.8209	1.0000							
<i>K. pneumoniae</i>	0.9291	0.9205	0.9337	0.9359	0.8312	1.0000						
log P	<b>0.8306</b>	<b>0.8294</b>	<b>0.8384</b>	<b>0.9269</b>	<b>0.7599</b>	<b>0.8638</b>	1.0000					
MD	-0.3675	-0.3141	-0.2808	-0.2217	0.0070	-0.2919	-0.3009	1.0000				
DH <sub>f</sub>	-0.1099	-0.1701	-0.6272	-0.6429	-0.6177	-0.5759	-0.2780	-0.1542	1.0000			
HOMO	0.2668	0.1715	0.1340	-0.0410	-0.0163	-0.0016	-0.0096	-0.4383	0.0870	1.0000		
Pot. Ion	-0.4028	-0.3325	-0.3145	-0.1256	0.0042	-0.2749	-0.3016	0.8944	-0.1634	-0.6378	1.0000	
LUMO	0.3665	0.2728	0.2648	0.0936	0.0299	0.2433	0.2716	-0.8993	0.1772	0.6628	-0.9676	1.0000

Table 5  
PLS analysis of the antimicrobial activity of N-alkylpyridinium compounds

Bacteria	q <sup>2</sup>	Ncomp	r <sup>2</sup>	S_ERR	F	n
<i>P. aeruginosa</i>	0.811	5	0.93	0.154	79.77	36
<i>E. coli</i>	0.602	2	0.707	0.394	61.54	61
<i>K. pneumoniae</i>	0.933	9	0.981	0.145	145.78	42
<i>B. subtilis</i>	0.635	2	0.756	0.502	74.33	55
<i>B. megaterium</i>	0.835	4	0.927	0.268	97.70	36
<i>S. aureus</i>	0.973	6	0.994	0.089	739.68	43

sidered, since the steric part of the pyridine moiety predicts that small groups are needed in order to increase activity. Hydrogen donors and hydrogen acceptors were used in an attempt to increase water solubility. According to predicted activity and feasibility of synthesis, compounds **3**, **10**, **14** and their C12 chain analogs **11**, **18**, and **12** were chosen for synthesis. The latter was considered because the control of MIC variability in the training set as well as the compounds showed a good profile: highest potency (reported log MIC = 6.0) and water solubility (log P = 5.51).

In addition, we decided to synthesize analogues of vitamin B6. These analogues also have the pyridine moiety in

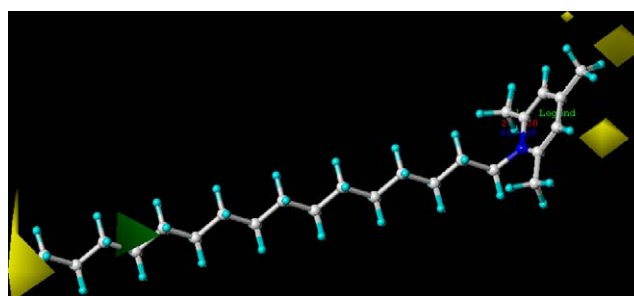


Fig. 1. CoMFA contours of the activity in *E. coli* in the alkylpyridinium series. Bioactive measurement increases when there is more bulk near green, less bulk near yellow, more electrostatic near red, and less electrostatic near blue.

addition to hydrophilic groups (two hydroxyl groups). Three different molecules were proposed and modeled to predict the activity. These are presented in Table 7. Although these compounds showed comparable antimicrobial predicted values, only compound **19** was selected and synthesized.

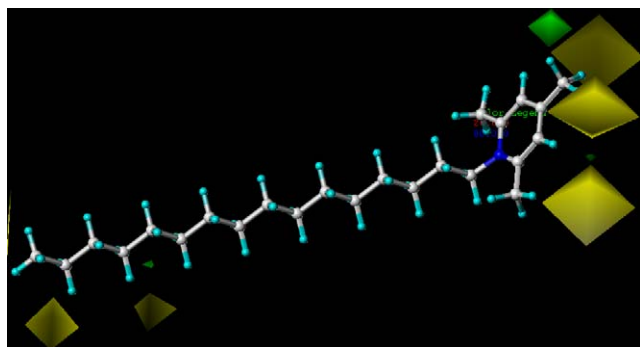


Fig. 2. CoMFA contours of the activity in *S. aureus* in the alkylpyridinium series. Bioactive measurement increases when there is more bulk near green, less bulk near yellow, more electrostatic near red, and less electrostatic near blue.

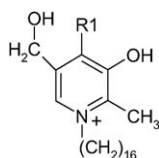
Table 6

CoMFA analysis prediction of the candidates designed. Compounds were modeled as data set for CoMFA

Compound		Predicted LOGMIC (M)			
Comp	Tail	Head	<i>E. coli</i>	<i>S. aureus</i>	
Nr.	No. C	Pyridine Subst.			
1	16C	2-acetyl	4.35	6.73	
2	16C	3-acetyl	4.61	6.15	
3	16C	4-acetyl	4.63	6.25	
4	16C	2-methoxy	4.73	6.81	
5	16C	3-methoxy	4.80	6.33	
6	16C	4-methoxy	4.67	6.38	
7	14C	2-methoxy	5.15	6.30	
8	16C	2-hydroxymethyl	5.27	6.57	
9	16C	4-hydroxymethyl	4.85	6.36	
10	16C	2,4,6-trimethyl	5.64	6.56	
11	12C	4-acetyl	5.95	5.56	
12	12C	2,4,6-trimethyl	6.02	5.95	
14	16C	4-(methoxymethyl)	5.08	6.35	
15	16C	4-[(methoxymethoxy)methyl]	5.00		
16	16C	4-[2-(methoxyethoxy)methyl]	5.15		
17	16C	4-{[2-(2-(ethoxyethoxy)ethoxy)methyl]}	4.87		
18	12C	4-(methoxymethyl)	4.59	5.89	

Table 7

Vitamin B6 analogues designed for CoMFA evaluation



Compound		Predicted LOGMIC (M)		
Comp Nr	Tail Nr C	R1	<i>E. coli</i>	<i>S. aureus</i>
19	16	-CH2-OH	5.19	6.31
20	16	CHO	5.14	6.14
21	16	-CH2-NH2	5.32	6.32

### 4.3. Chemistry

All the target compounds were synthesized, some of them in a low yield, due mainly to the elimination side reaction. Although these reactions have inherently low yields, modifi-

cations in temperature and alkylating reagent (from chloride to tosylate), allowed the synthesis of selected compounds in yields above 20%. In other cases, however, the accessibility of starting materials allowed the synthesis of adequate quantities of compounds despite low yields.

Compounds **3**, **10**, **14**, and **16** were obtained as tosylates, that were exchanged by the bromide after the flash chromatography purification. However, compound **19** did not exchange the tosylate group by this process.

### 4.4. Biology

After the synthesis, the log P of the compounds was determined using Hansch methodology. Table 8 shows the data obtained. Nearly all compounds tested presented lower log P than CPC. Only compound **3** had a higher log P.

MICs against *E. coli*, *S. aureus* and *S. typhimurium* are presented in Table 9. These were determined using CPC and ampicillin as a positive control. Due to the nature of the MIC, data in Table 9 shows a better correspondence with *S. aureus* predicted values, since MICs are lower than for *E. coli*. In these results the MIC presented is a range value where the actual activity is between the lower concentration which shows no growth and the next concentration where bacteria grow, according to the dilution scheme. So the variations in the residual values are higher in lower activity data. This was noted when a double dilution scheme was determined for *E. coli*. In order to establish the differences between compounds, a narrower dilution scheme was used. So, MICs in a range of 5- to 100 µg/ml against *E. coli* were tested and the obtained values presented in Table 9.

In this second dilution scheme, compound **10** showed slightly more activity than CPC. Note that **18** was as active as CPC, but is 7 times more hydrophilic, and probably could be easier to wash from the applied food. These results show that all the compounds were active, which validates the CoMFA model that was generated.

On the other hand, compound **12** was an outlier in the CoMFA model, it was retained because it was the alkylpyridinium analogue with the highest activity and a lower logP reported in the literature. This compound was used as an indicator of the variability on the training set. Structural data, as well as physical constants, confirmed the identity of **12**. Pre-

Table 8

Water Octanol partition coefficient (log P) determined for the alkylpyridinium compounds selected

Compound	LogP
3	2.712
10	1.569
11	1.006
12	0.527
14	nd
18	1.115
19	0.870
CPC	1.78 (1.77)

nd: no determined, (reported [23]).

Table 9

MIC data of the compounds synthesized over different microorganisms. The MIC values predicted by the CoMFA model are also presented

Comp	<i>E. coli</i>			MIC $\mu\text{g/ml}$ (LogMIC)			
	exp	pred	resid	<i>S. typhimurium</i>	<i>S. aureus</i>	pred	resid
<b>3</b>	15(4.45)	(5.077)	(-0.62)	64	0.40(6.02)	(6.25)	(-0.23)
<b>10</b>	5(4.93)	(5.24)	(-0.319)	25	0.10(6.62)	(6.56)	(0.06)
<b>11</b>	15(4.39)	(4.5)	(-0.11)	40	6.50(4.75)	(5.56)	(-0.81)
<b>12</b>	64(3.66)	(4.57)	(-0.91)		2.00(5.16)	(5.95)	(-0.79)
<b>14</b>	5(4.93)	(5.07)	(-0.14)	64	0.20(6.32)	(6.35)	(-0.03)
<b>18</b>	10(4.57)	(4.58)	(-0.01)	45	1.65(5.35)	(5.89)	(-0.54)
<b>19</b>	>50(3.87)	(5.18)	(-1.31)	>50	6.50(4.86)	(6.31)	(-1.45)
<b>CPC</b>	5(4.85)	(4.902)	(-0.05)	35	0.20(6.25)	(6.638)	(-0.39)
<b>Amp</b>	2			0.4	0.812		

liminary MIC determination showed a lower activity, actually better predicted by the CoMFA model, which was later confirmed by a second laboratory. The use of a different strain might, perhaps, explain the data obtained, since ampicillin and CPC are in the range reported [3,5,24].

Based in the log P and the activity determined, we will select candidates for the next phase of the study were their residual analysis will determined in different food as chicken, meat and fruits.

## 5. Conclusions

The alkylpyridinium compounds show a relationship with the log P parameter, but computationally it is difficult to predict log P for alkylpyridinium compounds. It is in these cases where 3D-QSAR is helpful in the design of new potential candidates. Models created with CoMFA were statistically significant and showed that the activity is highly correlated with the steric part in the chain, and surprisingly also in the pyridine moiety. Based in these contours, 7 derivatives were designed and synthesized and their structure was elucidated by NMR, MS and IR spectroscopy. All of the compounds presented a good activity, especially compound **10**. The activity determination validated the CoMFA model generated.

## 6. Experimental

### 6.1. Chemistry

Compounds were synthesized according to the general procedure described before. Specific quantities, conditions and results are given next to each compound.

#### 6.1.1. 1-Hexadecyl-4-acetylpyridinium bromide (3)

2.40 mL (2.24 g, 0.0220 mol) of 4-acetylpyridine, 8.4 g (0.0220 mol) cetyl tosylate, and 200 mL acetonitrile. 23 h at 130 °C. Crude compound was recrystallized from acetone ether mixture, crystallized as a pale yellow solid (1.5 g, 37% yield), mp 88–89.3 °C. IR: 3854.86 ( $\text{N}^+$ ), 3101, 2915, 2848, 1455 (CH sat), 1702 (C=O), 3023, 1634 (ArCH), 3443 (OH, monohydrate).  $^1\text{H-NMR}$ : 9.67 (dd, 2H,  $J=6$  Hz) 8.52 (dd, 2H,  $J=6$  Hz), 5.058 (t, 2H,  $^+\text{N-CH}_2$ ) 2.80 (s, 3H,  $\text{CH}_3\text{-C=O}$ )

2.05 (m, 2H,  $^+\text{N-CH}_2\text{-CH}_2$ ), 1.233 (m, 26H, H chain) 0.861 (t, 3H,  $\text{CH}_3$  chain). Elemental analysis: Calculated: %C: 71.26, %H: 10.25, %N: 3.96; found: %C: 71.28, %H, 10.24, %N: 3.86).

#### 6.1.2. 1-Dodecyl-2,4,6-trimethylpyridinium bromide (12)

4.20 mL (3.60 g, 0.01309 mmol) of dodecyl bromide, 3.5 mL (3.205 g, 0.02618 mmol) collidine, 1% of Potassium iodide as catalyst. Mix was heated at 90 °C for 24, then 50 mL of acetonitrile was added and refluxed for 14 days. Compound **12** was recrystallized from ethyl acetate, giving white leaves, mp 92–94 °C. IR: 3668.16 ( $\text{N}^+$ ), 3201, 2918, 2850 (CH sat), 3030 (ArCH), 3352 ( $\text{H}_2\text{O}$ ).  $^1\text{H-NMR}$ : 7.6 (s, 2H, Harom), 4.6 (m, 2H,  $^+\text{N-CH}_2$ ), 2.95 (s, 6H,  $\text{CH}_3$  arom<sub>ortho</sub>) 2.55 (s, 3H,  $\text{CH}_3$  arom<sub>meta</sub>), 1.98 (s, 1H,  $^+\text{N-CH}_2\text{-CH}_2$ ), 1.78 (m, 2H,  $^+\text{N-CH}_2\text{-CH}_2\text{-CH}_2$ ), 1.45 (m, 2H,  $^+\text{N-CH}_2\text{-CH}_2\text{-CH}_2\text{-CH}_2$ ) 1.13 (m, 14H,  $\text{CH}_2$  sat chain), 0.92 (s, 3H,  $\text{CH}_3$ ).  $^{13}\text{C-NMR}$ : 157 (C2,6 pyridine), 154 (C4 pyridine), 129.03 (C3,5 pyridine), 53.55 ( $^+\text{N-C}$ ), 31.72 (C2 chain), 29.40 (C10 chain) 29.28 (C5,6 chain), 29.21 (C7 chain), 29.13 (C8 chain) 28.95 (C9 chain), 28.73 (C4 chain), 26.67 (2  $\text{CH}_{3\text{ortho}}$  pyridine ring), 22.49 (C3 chain), 21.64 (C11 chain), 21.49 ( $\text{CH}_{3\text{para}}$  pyridine ring), 13.91 (C12 chain). Elemental analysis. Calculated: %C: 64.83, %H: 9.80, %N: 3.78; found %C: 64.63, %H: 10.13, %N: 4.00)

#### 6.1.3. 1-Dodecyl-4-acetylpyridinium bromide (11)

3.3 mL (3.083 g, 0.0270 mol) of 4-acetylpyridine, 6.7 mL (7.22 g, 0.0270 mol) dodecyl bromide, 50 mL of acetonitrile, heated at 100 °C for 27 h. **11** was recrystallized from ethanol/ether, to give pale yellow solid (mp 82–83 °C). IR: 3668.16 ( $\text{N}^+$ ), 3201, 2912, 2841, 1460 (CH sat), 1705 (C=O) 3048, 1634 (ArCH) 3456 (OH monohydrate).  $^1\text{H-NMR}$ : 9.7 (dd, 2H arom.,  $\text{H}_{\text{ortho}}$  pyridine,  $J=6$  Hz), 8.60 (dd, 2H arom.,  $\text{H}_{\text{meta}}$ ,  $J=6$  Hz.) 5.0 (t, 2H,  $^+\text{N-CH}_2$ ) 2.8 (s, 3H,  $\text{CH}_3$  acetyl) 2.01(m, 2H,  $^+\text{N-CH}_2\text{-CH}_2$ ), 1.13 (m, 10H,  $\text{CH}_2$  chain), 0.92 (s, 3H,  $\text{CH}_3$ ).  $^{13}\text{C-NMR}$ : 198.20(carbonyl) 148.20 (C2,4 pyridine), 146.87 (C4 pyridine) 126.52 (C5,3 pyridine), 61.425 ( $^+\text{N-C}$ ), 31.78 (C2 chain), 31.68 (C10 chain), 29.39, (C5,6 chain), 29.31 (C7 chain), 29.17 (C8 chain), 29.12 (C9 chain) 28.89 (C4 chain), 27.43 (C3 chain), 25.94 ( $\text{CH}_3$  acetyl group), 22.45 (C11 chain) 13.88 (C12 chain). Element-



tal analysis: calculated %C: 61.62, %H: 8.71, N: 3.78; found: %C: 61.68, %H: 8.70, %N: 3.99).

#### 6.1.4. 1-hexadecyl-2,4,6-trimethylpyridinium Bromide (10)

12.6 g (0.0317 mol) cetyl tosylate, 4.8 mL (4.33 g, 0.0360 mol) 2,4,6-collidine, 150 mL acetonitrile, heated at 100 °C for 9 days. Compound **10** was recrystallized from acetone/ether, giving white needles with a melting point of 106.3–106.9 °C. <sup>1</sup>H-NMR: 7.6 (s, 2H, Harom), 4.6 (t, 2H, +N-CH<sub>2</sub>), 2.95 (s, 6H, CH<sub>3</sub> arom<sub>orto</sub>) 2.55 (s, 3H, CH<sub>3</sub> arom<sub>para</sub>), 1.76 (sext, 1H, +N-CH<sub>2</sub>-CH<sub>2</sub>), 1.53 (sext, 2H, +N-CH<sub>2</sub>-CH<sub>2</sub>-CH<sub>2</sub>), 1.4–1.2 (m, 22H, CH<sub>2</sub> chain), 0.88 (s, 3H, CH<sub>3</sub>). <sup>13</sup>C-NMR: 157 (C2,6 pyridine), 154 (C4 pyridine), 129.03 (C3,5 pyridine), 53.45 (+N-C), 31.8 (C2 chain), 29.55 (C10 chain) 29.361 (C5,6 chain), 29.21 (C7 chain), 29.13 (C8 chain) 28.95 (C9 chain), 28.73 (C4 chain), 21.68 (2 CH<sub>3</sub><sub>ortho</sub> pyridine ring), 22.49 (C3 chain), 22.57 (C11 chain), 21.59 (CH<sub>3</sub><sub>para</sub> pyridine ring), 14.01 (C16 chain). Elemental analysis: calculated %C: 67.58, %H: 10.40, %N: 3.28; found %C: 67.92, %H: 10.89, %N: 3.25

#### 6.1.5. 1-Dodecyl-4-methoxymethylenepyridinium bromide (18)

5 mL (4.67 g, 0.01947 mol) dodecyl bromide, 2 g (0.01623 mol) of 4-methoxymethylenepyridine (**22**) and 150 mL of acetonitrile, heated at 120 °C for 3 days. Target compound was obtained as white needles with a melting point of 69–70 °C. <sup>1</sup>H-NMR: 9.46 (d, 2H, H arom, 2,6-pyridine), 8.05 (d, 2H, H arom, 3,5-pyridine), 4.97 (t, 2H, +N-CH<sub>2</sub>), 4.75 (s, 2H, CH<sub>2</sub>-O), 3.53 (s, 3H, CH<sub>3</sub>-O), 2.02 (sext, 2H, +N-CH<sub>2</sub>-CH<sub>2</sub>), 1.4–1.2 (m, 18H, CH<sub>2</sub> chain), 0.875 (s, 3H, CH<sub>3</sub>). MS-FAB+: 292 (m/e, M<sup>+</sup>) corresponding to pyridinium cation. Elemental analysis: calculated: %C: 61.28, %H: 9.20, %N: 3.76; found %C: 61.15, %H: 9.51, %N: 4.12

#### 3.1.6. 1-Hexadecyl-4-methoxymethylenepyridinium bromide (14)

5.9 ml (4.67 g, 0.01850 mol) cetyl tosylate, 2 g (0.01623 mol) of 4-methoxymethylpyridine (**22**) and 150 ml acetonitrile, heated at 130 °C for 2 days. Compound **14** was obtained after elution, white needles, mp 72–76 °C. <sup>1</sup>H-NMR 9.38 (d, 2H, Harom, 2,6-pyridine), 8.06 (d, 2H, Harom, 3,5-pyridine), 4.97 (t, 2H, +N-CH<sub>2</sub>), 4.75 (s, 2H, CH<sub>2</sub>-O), 3.53 (s, 3H, CH<sub>3</sub>-O), 2.02 (sext, 2H, +N-CH<sub>2</sub>-CH<sub>2</sub>), 1.4–1.2 (m, 26H, CH<sub>2</sub> sat chain), 0.875 (s, 3H, CH<sub>3</sub>).

#### 6.1.7. 1-Hexadecyl-4-hydroxy-3,4-bis(hydroxymethyl)-2-methylpyridinium tosylate (19)

4 g (0.01945 mmol) of pyridoxine hydrochloride was dissolved in 250 ml of ethanol with stirring under nitrogen, 1.09 g (0.01945 mol) of KOH (previously dissolved in 25 ml of ethanol) was added. After 1 h, the mixture was concentrated over vacuum, and the solid was transferred to the Parr reactor where 7.7 g (0.01945 mol) of cetyl tosylate plus 100 ml of acetonitrile were added and the mixture heated at 120 °C for 6 h.

The white solid obtained was recrystallized from acetone/ether. Compound **19** was obtained as pale yellow needles with a melting point of 118–120 °C. <sup>1</sup>H-NMR: 8.06 (s, 1H, Harom, Hpyridine), 7.45(d, 2H, Harom, *orto* sulphonate, TSO-), 7.05(d, 2H, Harom, *orto* methyl of tosylate-), 5.740 (s, 1H, HO-pyridoxine), 4.798 (s, 2H, Ar-CH<sub>2</sub>-O pyridoxine), 4.67 (s, 2H, Ar-CH<sub>2</sub>-O pyridoxine), 4.52 (t, 2H, +N-CH<sub>2</sub>), 2.617 (s, 3H, CH<sub>3</sub>-arom, tosylate), 2.271 (s, 3H, CH<sub>3</sub>-arom, pyridoxine), 1.760 (sext, 2H, +N-CH<sub>2</sub>-CH<sub>2</sub>), 1.284–1.20(m, 26H, CH<sub>2</sub> sat chain), 0.838 (s, 3H, CH<sub>3</sub>). MS (FAB<sup>+</sup>) presented M<sup>+</sup> corresponding to the expected pyridinium cation (M/z = 394). Elemental analysis: calculated: %C: 65.81, %H: 9.09, %N: 2.48, %S 5.67; found %C: 65.68, %H: 9.14, %N: 2.52.

## 6.2. Computational Studies

Molecular modeling studies were performed on a Silicon Graphics Octane 2 workstation, using SYBYL 6.8 molecular modeling software from Tripos Inc., St. Louis, MO (Tripos, 2002).

### 6.2.1. Molecular 3D Structure Building

For the QSAR study, the structure of the compounds were obtained from the Cambridge Crystallographic Database as implemented in Unity 4.1 or by small modifications of the structure available in the database using Sybyl 6.8. All of the analogues were minimized by the PM3 semiempirical Hamiltonian in Mopac 6.0 package in Sybyl (keywords used: Precise, Full, Mullik and in some cases MMOK).

### 6.2.2. Alignment Rule

For the 3D-QSAR studies, the structures were aligned using the Match command in Sybyl. CPC was the template and the atoms selected for the rms fitting are marked with an asterisk (\*) in Fig. 3. MOPAC charges were retrieved from the PM3 file for each molecule.

### 6.2.3. COMFA analyses

3D-QSAR analyses were performed using the Comparative Molecular Field Analysis (CoMFA) program, as implemented in Sybyl. CoMFA fields were calculated using a positive charge and a carbon sp<sup>3</sup> as electrostatic and steric probes, respectively. Steric and electrostatic interactions were calculated using Tripos Force field with a distance-dependent dielectric constant at all intersections in a regular spaced (2 Å) grid. The minimum σ (column filtering) was set to 2 Kcal/mol, with a cutoff of 30 Kcal/mol.

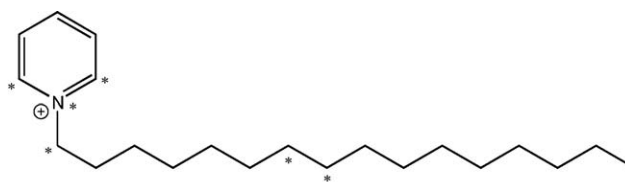


Fig. 3. CPC molecule where asterisk mark shows the atoms selected for the Atom Based Alignment.

### 6.2.4. PLS Analysis

The CoMFA models were developed using partial least-squares (PLS) by following the standard implementation in Sybyl. The different descriptor blocks have been scaled to each other using CoMFA standard scaling option. To check the statistical significance of the models, cross-validations were done by means of the leave one out (LOO) procedure. The results from the cross-validation analysis were expressed as the cross-validated  $q^2$  ( $r^2_{cv}$ ). It is defined as  $r^2_{cv} = 1 - \text{PRESS} / \sum (Y - Y_{\text{mean}})^2$  where  $\text{PRESS} = \sum (Y - Y_{\text{pred}})^2$ . The optimum number of components was determined by selecting the smallest  $s_{\text{press}}$  value.  $S_{\text{press}}$  value is the root mean predictive error of the sum of the squares. It is the expected uncertainty in the prediction for the individual compounds in the set.  $S_{\text{press}} = (\text{PRESS} / (n - c - 1))^{1/2}$  where  $n$  is the number of rows and  $c$  is the number of components. Usually the standard smallest  $S_{\text{press}}$  value corresponds to the highest  $r^2_{cv}$ . The optimal number of components was subsequently used to derive the final QSAR models. For conventional analysis (not cross validated) the minimum  $\sigma$  standard deviation threshold (column filtering) was set to 2 Kcal/mol to improve the signal-noise ratio. The  $r^2_{cv}$ ,  $S_{\text{press}}$ ,  $r^2$ , and SE values were computed as defined in SYBYL. SE is the standard error of the estimate. It is the measure of the target property uncertainty still unexplained after the QSAR has been derived.

### 6.3. Biology

#### 6.3.1. Partition coefficient (log P) determination

Log P was measured using the guidelines of Hansch and Leo [23]. Stock solutions (0.1, 0.5, and 1 mg/mL) of each compound were prepared. Then 1 mL of each solution was dissolved in 20 mL of deionized water (presaturated overnight with octanol) in a centrifuge tube. Then 1 mL of octanol (presaturated overnight with water) was added. The centrifuge was shaken for 1 hour at 150 rpm at 30 °C. The layers were separated at 1500 rpm, and the amount of compound in the aqueous layer measured. A graph of concentration of the compound in octanol vs concentration in water was prepared, and the log of the slope is log P value.

#### 6.3.2. Antimicrobiological activity

The macrodilution susceptibility test in Muller-Hinton Broth (GIFCO) was used for the determination of antibacterial activity [24]. The utilized test organisms were: *Salmonella typhimurium* ATCC 14028, *E. coli* ATCC25922 *S. aureus* ATCC29123. Ampicillin and CPC were used as standard antibacterials. Solutions of the test compounds, ampicillin and CPC prepared in phosphate buffer (pH= 7.0) and deionized water at concentration of 512 mg mL<sup>-1</sup>. The two fold dilutions of the compounds were prepared (256, 128, ..., 6.25 mg mL<sup>-1</sup>). The microorganism suspensions at 10<sup>6</sup> CFU mL<sup>-1</sup> (Colony Forming Unit mL<sup>-1</sup>) concentration were inoculated into the corresponding test tube. Plates were incubated at 38 °C for 24 h. The incubation chamber was kept sufficiently humid. At the end the incubation period, the MICs

were determined controls for the DMSO, solvents, microorganisms and media microorganisms were also done (Table 9).

### Acknowledgements

Sergio Rodríguez-Morales is grateful to the PhD thesis scholarships from the National Council of Science and Technology, Mexico, and from the Graduate Studies General Board, National Autonomous University of Mexico.

### References

- [1] Report of Economical research services, U. S. Agricultural Department, web site. Available from: <http://www.econ.ag.gov/briefing/foodsafte>.
- [2] M. McCoy, Chem. Eng. News 6 (1998) 21–41.
- [3] P.J. Breen, C.M. Compadre, E.K. Fifer, H. Salari, D.C. Serbus, D.L. Lattin, J. Food Sci. 6 (1995) 1191–1196.
- [4] P.J. Breen, H. Salari, C.M. Compadre, J. Food Pro. 60 (1997) 1019–1021.
- [5] H. Kourai, K. Tatechi, T. Horie, K. Takeichi, I. Shibasaki, J. Antibact. Antifung. Agents 13 (1983) 245–253.
- [6] J. Lin, S. Qiu, K. Lewis, A.M. Klivanov, Biotechnol. Prog. 18 (2002) 1082–1086.
- [7] J.C. Tiller, S.B. Lee, K. Lewis, A.M. Klivanov, Biotechnol. Bioeng. 79 (2002) 465–471.
- [8] J.C. Tiller, C.J. Liao, K. Lewis, A.M. Klivanov, Proc. Natl. Acad. Sci. USA 98 (2001) 5981–5985.
- [9] H. Kourai, T. Horie, K. Takeichi, I. Shibasaki, Bokin Bobai 8 (1980) 191–199.
- [10] H. Kourai, F. Machicawa, K. Tateishi, T. Horie, K. Takeichi, I. Shibasaki, J. Antibact. Antifung. Agents 11 (1983) 553–562.
- [11] Q. Zhu, Z. Guo, N. Huang, F. Chu, J. Med. Chem. 40 (1997) 4319–4328.
- [12] Y.B. Li, M.F. Slavik, J.T. Walker, H. Xiong, J. Food Sci. 62 (1997) 605–607.
- [13] R.S. Shelton, C.H. Van Campen, L. Lang, J. Am. Chem. Soc. 68 (1946) 753–75911.
- [14] T.I. Oprea, C. Waller, Reviews in Computational Chemistry, in: Boyd and LipKowitz, VCH. Pub, 1997 Vol XI.
- [15] G. Greco, E. Novellino, Y.C. Martín, Reviews in Computational Chemistry, in: Boyd and LipKowitz, VCH. Pub, 1997 Vol XI.
- [16] Y.M. Martin, K.H. Kim, T.C. Lin, in: Advances in Quantitative Structure Property Relationships, Charton, JAI Press, Greenwich, CT, 1996 Vol. 1 Chapter 1.
- [17] U. Thibaut, G. Folkers, G. Klebe, H. Kubinyi, A. Merz, D. Rognan, in: H. Kubinyi (Ed.), 3D-Qsar in Drug Design: Theory Methods and Applications, Kluwer Academic Publishers, 1993 Vol 1.
- [18] G. Folkers, A. Merz, D. Rognan, in: H. Kubinyi (Ed.), 3D-Qsar in Drug Design: Theory Methods and Applications, Kluwer Academic Publishers, 1993 Vol 1.
- [19] T. Maeda, S. Goto, Y. Manabe, K. Okazaki, H. Nagamune, H. Kourai, Biocontrol Sci. 1 (1996) 41–49.
- [20] H. Kourai, Y. Hasegawa, K. Wada, J. Antibact. Antifung. Agents 22 (1994) 653–661.
- [21] F. Devinsky, I. Lacko, E. Nlyncik, E. Svajdleka, V. Borovska, Pharmazie 51 (1996) 727–731.
- [22] L.H. Bluhm, T. Li, Tetrahedron Lett. 39 (1998) 3623–3626.
- [23] C. Hansch, A. Leo, Exploring QSAR: Fundamentals and Applications in Chemistry and Biology, ACS Pub, 1995.
- [24] A. Waitz, et al., in: NCCLS, 10, 1990 M7-A2.
- [25] J.E. Lien, C. Hansch, M.S. Anderson, J. Med. Chem. 11 (1968) 430–441.